8. Efficient mode coupling technique between photonic crystal heterostructure waveguide and silica waveguides

A paper was submitted to Optics Letter, 2004/04/08, in peer review

8.1 Introduction

Photonic crystals (PCs) can be severed for various micro-optical components and microcircuits[1,2,3,4,5], for example, planar photonic crystal waveguides (PPCWGs) [6,7,8] have been widely applied to used to guide light in terms of line defects. To construct efficient optical integrated circuits (OICs), it is necessary that the coupling efficiency between different partial components arrives as high as possible because losses occur at the junctions forming by different parts. For instance, PPCWGs have to connect to the conventional silica waveguides (SWGs) at their entrance and exit ends as for a practical optical communication element. In this case, acquiring optimal power conversion among the external wires and the PPCWGs still continues to be a challenge, for instance, enlarging the band gap size, promoting the transmission efficiency, and reducing back-reflections arising from mode mismatching at interfaces owing to different propagation properties of light waves in SWG and PPCWGs and their different widths.

Inspired by these active issues, in this letter, we propose planar photonic crystal heterostructure waveguide (PPCHWG) consisting of two semi-infinite PCs with different structural parameters, which is connected to two external SWGs. PPCHWGs possess the ability of flexible control of the defect states by adjusting the structural parameters of two component PCs in heterostructure. Unlike the conventional two-dimensional PCWGs formed by the removal of some rods or air holes in lines (thus, the width of the WGs is determined by the number of the defect lines), the PPCHWGs are formed by introducing relatively longitudinal gliding of the cylinders in the lattices on the two sides of the interface of heterostructure (referred to the longitudinally gliding of lattices) or displacing the cylinders in the lattices on the either sides of the interfaces (referred to the transverse displacement of lattices). Therefore, the width of the PPCHWGs can be engineered for acquiring optimal coupling efficiency. We report the typical design of the efficient mode coupling between PPCHWG and SWGs.

8.2 Structure and coupling techniques

Recently, it has proven theoretically that omni-directional total reflection frequency range can be significantly enlarged by combining two or more one-dimensional (1D) PCs, whose omni-directional PBGs may be bridged to connect each other [9]. Inserting multiple photonic quantum-wells into PCs can generate the defect modes in the omnidirectional PBGs [10]. We consider a typical PPCHWG connected to two external SWGs, as sketched in Fig. 8.1. The 2D photonic crystal heterostructure is composed of two-semi-finite PCs, which are a square lattice of dielectric circular rods of *GaAs* (its refractive index is n = 3.4 at wavelength ¸ = 1.55 μm) in air background with lattice constant a and different rod radii (r_1 and r_2), i.e., different filling fractions (f_1 and f_2).

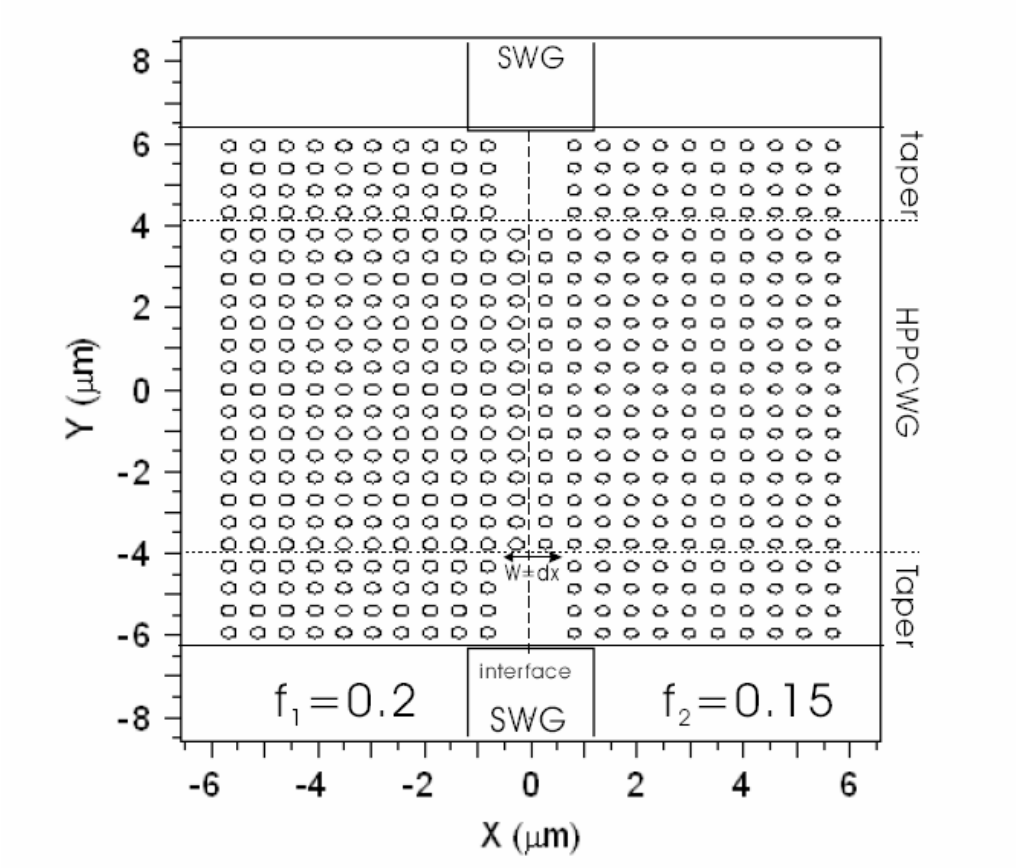

Fig. 8.1 Schematic view of a heterostructure planar photonic waveguide formed by two semi-infinite square lattices with different filling fractions of cylinders combined with a stepwise planar photonic crystal taper for input and output couplings.

The SWG consists of silica with a dielectric index of 145 and a width of 2.5 μm, surrounded by air. The PPCHWG and SWG both are lied on the *x*-*y* plane and the normal direction of the interface is parallel to the *x*-axis. To acquire the optimal mode coupling between the PPCHWG and SWG, the suggested coupling structures at the entrance and exit terminals of the PPCHWG is shown in Fig. 8.1, by removing four rods on the either sides of the interface of the PPCH along the *y*-direction, in one line and from two ends. By using the plane-wave expansion [11] method with a combination of supercell technique, we calculate the photonic band gaps (PBGs) and find that the PBG lied at the ranges of a/λ *in* [0.262, 0.377] or λ in [1.432,2.06] μm along the Γ-*X* direction for the TM polarization. The parameters are chosen as : $f_1 = 0.2$, (i.e., $r_1 = 136nm$), and $f_2 = 0.15$, (i.e., $r_2 = 118nm$); $a = 540nm$. As reported in Refs.[12] and [13, 14], any guided modes can not be generated when not introducing relatively longitudinally gliding or transverse displacement of lattices together with cylinders on the either sides of the interface of PPCH to the host medium.

8.3 Results and discussion

It is desirable for serving as waveguides to produce the guided modes in the PBGs. Thus, we now introduce a relatively transverse displacement operation for the lattices together with cylinders on the either sides of the interface of heterostructure to the host medium by a distance of $dx = 1.42a$. The calculated photonic band structures are displayed in Fig. 8.2. For the TM polarization of the incident electromagnetic (EM) waves, a single guided mode is generated now. The distributions of the relevant EM fields are also shown in the insert of this figure for reference. It is evident that the guided modes exhibit strong localization behavior in the *x*-direction, i.e., perpendicular to the interface of the PPCH. These guided modes can be used for the waveguides.

To become a practical element of WGs, it requires to connect the PPCWGs to the external SWGs at the entrance and exit terminals of the PPCWG and to have high power conversional efficiency. We now focus on this issue. Recently, the planar photonic crystal (PPC) coupling techniques by varying the rod sizes for between PPC waveguides of different widths[15, 16] have been proposed. Furthermore, a coupling technique based on setting several defect rods [17, 18] within the conventional PPC tapers. Although high transmission was achieved with the transmission peaks exceeding 80% at certain localized frequencies, in

practice, it is difficult to control the rod size with required accuracy. Thus our tactics is to maximize the transmission efficiency between SWG and HPPCWG by using no defect pairs in the PPC tapers.

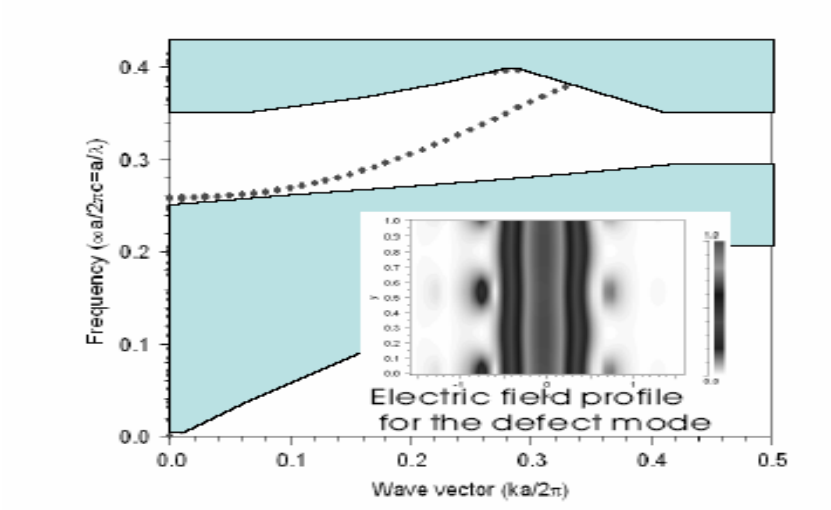

Fig. 8.2 The corresponding projected band structure and defect mode for the system composed of dielectric cylinders in air, which created by separating two semi-infinite lattices with the interface displacement of 1.42a. The parameters of the system are a = 540nm, f_1=0.2, f_2=0.15, and n=3.4, and EM waves are assumed to be polarized in the TM mode.

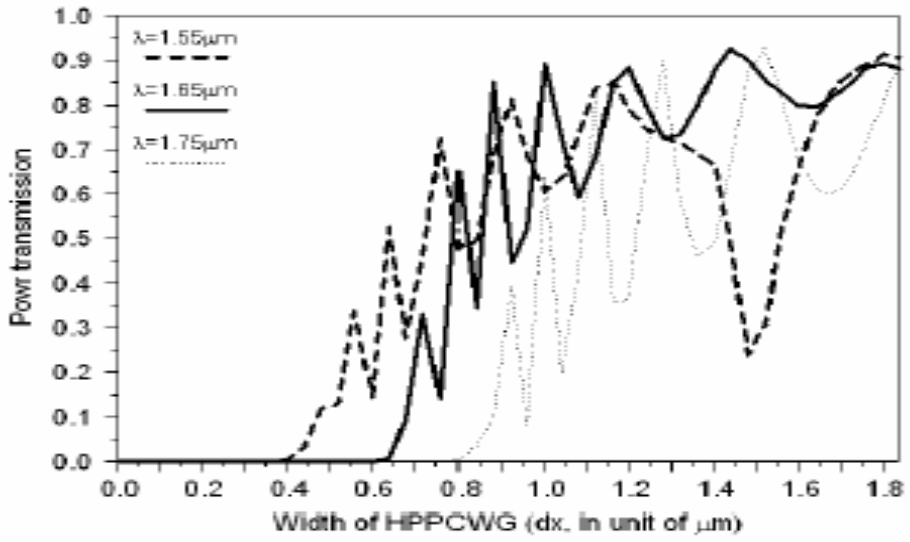

Fig. 8.3 The optimum displacement created by slipping two semi-infinite lattices relative to each other was obtained by varying the distance along the (1 0) direction has been optimized at the centered wavelength of λ=1.55 μm(dashed line),λ=1.65 μm (solid line) and λ=1.75 μm (dotted line), respectively. The transmission is measured at output end of SWG of a monochromatic continuous-wave with normalized power.

To gain the mode coupling with high conversion efficiency between the PPCHWG and SWG, the suggested coupling structures at the entrance and exit terminals of the PPCHWG is shown in Fig. 8.1, by removing four rods on the either sides of the interface of the PPCH along the *y*-direction, in one line and from two ends. We compute the transmittivity of system in terms of 2D finite-difference time-domain (FDTD) algorithm[19]. We assume that a TM polarized Gaussian wave packet with appropriate waveguide mode pattern is launched normally into the entrance terminal of the PPCHWG from the SWG. Perfectly matched layer (PML) conditions have been adopted to prevent unwanted reflections occurring [20]. The transmission spectrum of the system is obtained from the Fourier transformed time series and normalized with respect to the launched source. To find the optimal mode coupling conditions, we now change the relatively transverse displacement of the lattices of the either sides of interface of heterostructure, i.e., *dx*, for different operating wavelengths. The calculated power transmission as a function of the width of PPCHWG, i.e., *dx*, is shown in Fig. 8.3. Three different operation wavelengths are assumed : the dashed- (solid-, dotted-) curve corresponds to the fundamental mode of the SWG is excited by a sinusoidal monochromatic continuous wave with a normalized power in the y-direction(see, Fig. 8.1)[21]. The transmission is measured at output end of SWG. It is clearly seen from Fig. 8.3 that there exist a onset threshold of the PPCHWG width ($w = dx$) below which the transmission becomes zero because no any guide mode survives inside the range of the PBG on PPCH. As increasing the width of the PPCHWG, the transmission is rapidly increased in heavy oscillatory manner. The occurrence of these peaks in curves can be attributed to the formation of the resonance cavity formed by two Febry Perot-like PC mirrors at the interface of heterostructure. As increasing the operation wavelength, the onset of the transmission is shifted toward the large width region. The better performance with an average transmission level of 73.83% is achieved over the width range $w\ in\ \ [1.143, 1.83]\ \mu m$ and the maximum transmission is up to 93% for the operation wavelength $\lambda = 1.65\ \mu m$.

To further explore the merits of these coupling systems, we show the variations of the transmission spectrum of a HPPCWG as a function of the wavelength for five different widths : $w = dx = 0.5\ \mu m$ for the solid curve, $0.7\ \mu m$ for the dashed curve, $1.0\ \mu m$ for the dotted curve, $1.3\ \mu m$ for the long-dashed curve, and $1.44\ \mu m$ for the dash-dotted curve, respectively. (using the optimal center wavelength of ¸ = $1.65\ \mu m$ obtained before). The fundamental mode of the SWG is excited by a pulse wave, propagating along the *y*- axis. The

transmission spectrum is calculated with the overlap integral between the launched and measured fields at the exit end of the SWG. It is evident from Fig. 8.4 that all the curves oscillate with ¸ containing series of sharp peaks. There exists a cut-off wavelength for each given width of the PPCHWG. The lower the cut-off wavelength, the narrower the PPCHWG width is. As increasing the width of the PPCHWG, the amplitude of the oscillations is reduced and the average level of the transmission is significantly raised. The maximal transmittance can reach as high as 93% when the width $w = dx = 1.44\,\mu m$ of the PPCHWG. We also plot the field distributions in the entire structure with the width $w = 1.44\,\mu m$ of the PPCHWG in Fig. 8.5. It is obvious that a good coupling between the PPCHWG and SWG is achieved when the proposed coupling technique is employed.

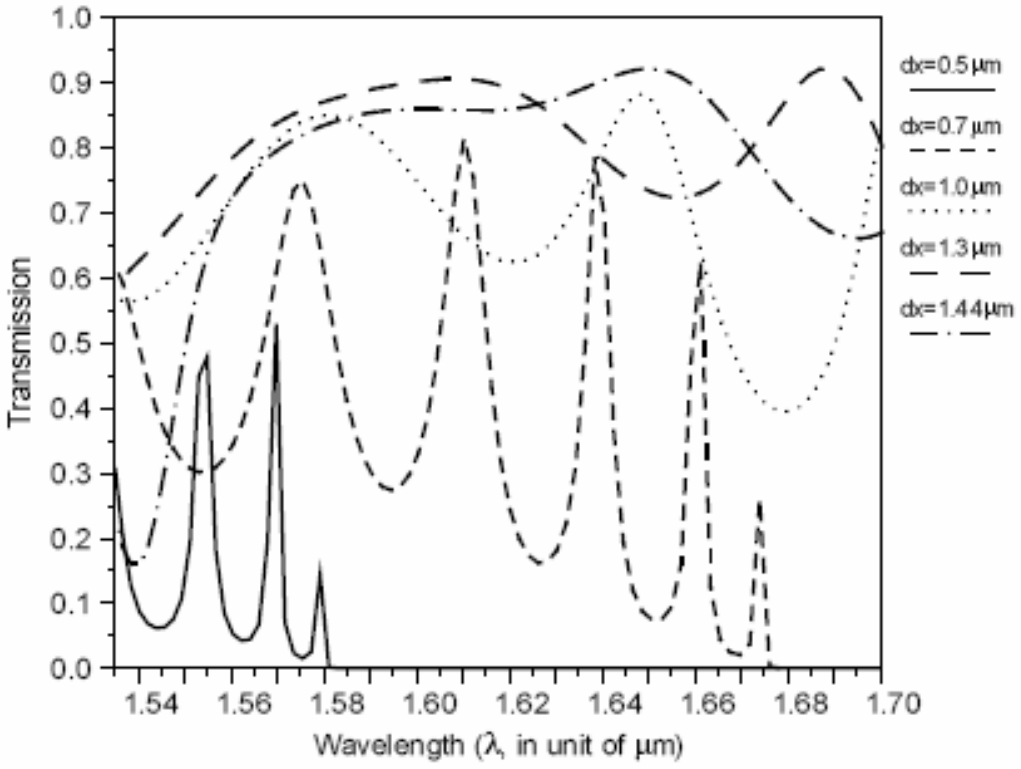

Fig. 8.4 The transmission spectrum of a HPPCWG of five different widths (w=dx), dx=0.5 μm (solid), dx=0.7 μm (dashed), dx=1.0 μm (dotted), dx=1.3 μm (long dashed) and dx=1.44 μm (dash-dotted) using the optimum center wavelength of $\lambda = 1.65\,\mu m$ obtained previously, couple to an input and output SWG. The fundamental mode of the SWG is excited by a pulsed wave and the transmission spectrum is calculated with the overlap integral between the launched and measured field at output SWG.

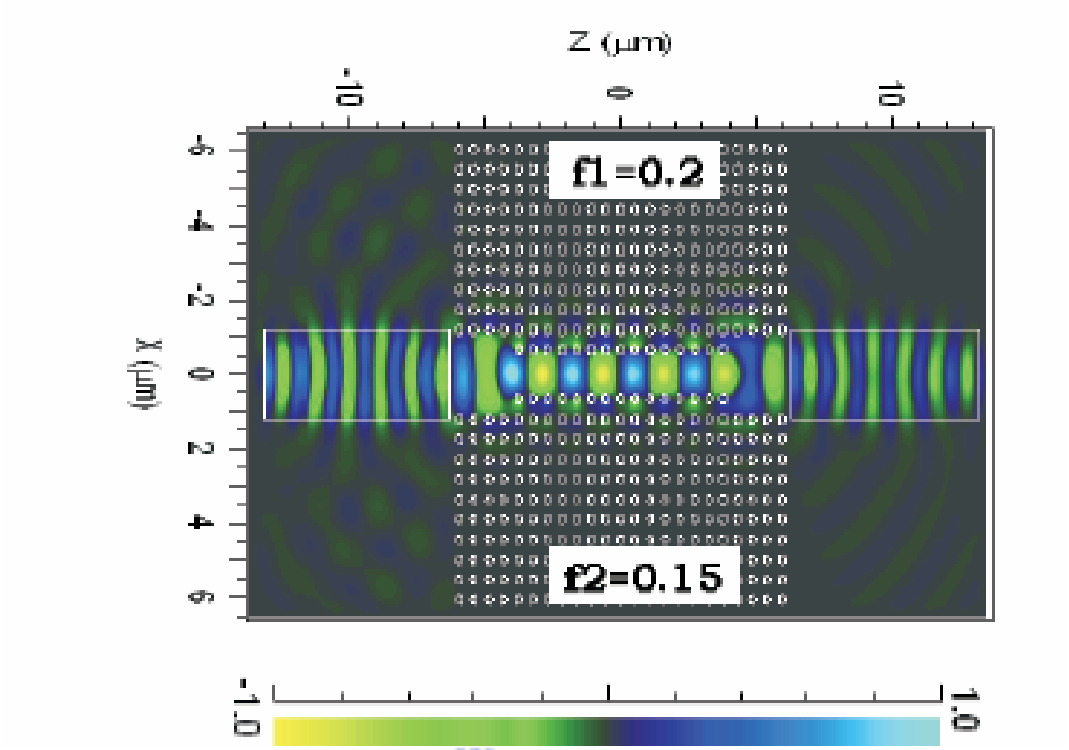

Fig. 8.5 The field distribution in the entire structure with the width of HPPCWG is w=dx=1.44 μm.

8.4 Summary

In conclusion, the coupling efficiency can be improved for mode matching from a SWG to a HPPCWG. By calculating the transmittance at the output end of SWG, we found the proposed structure to have high coupling efficiency and fabrication tolerance. The maximum transmittance exceeds 90% for a wavelength near 1.65 μm. It is worth noting that the HPPCWGs used in coupling process is achieved high transmission efficiencies without containing any pair of defects for mode matching at the entrance and exit terminals of HPPCWGs. Besides, the width of PPCHWGs can be flexibly controlled by adjusting the lateral separation of two component PCs in PC heterostructures.

Reference

[1] H. Kosaka,T. Kawashima, A. Tomita, M. Notomi, T. Tamamura, T. Sato, and S. Kawakami, Appl. Phys. Lett. 74, 1370-1372 (1999)

[2] H. Kosaka,T. Kawashima, A. Tomita, M. Notomi, T. Tamamura, T. Sato, and S. Kawakami, Appl. Phys. Lett. 74, 1212-1214 (1999)

[3] A. R. McGurn, Phys. Rev. B 61, 13235-13249 (2000)

[4] H. Kosaka,T. Kawashima, A. Tomita, M. Notomi, T. Tamamura, T. Sato, and S. Kawakami, Phys. Rev. B 58, 10096-10099 (1998)

[5] M. Tokushima, H. Kosaka, A. Tomita, and H. Yamada, Appl. Phys. Lett. 76, 952-954 (2000)

[6] A. Talneau, Ph. Lalanne, M. Agio and C.M. Soukoulis, Opt. Lett. 27, 1522-1524 (2002).

[7] P. Sanchis, J. Marti, J. Blasco, A. Martinez and A. Garcia, Opt. Express 10, 1391-1397 (2002).

[8] Jianhua Jiang, Jingbo Cai, Gregory P. Nordin, and Lixia Li, Opt. Lett. 28, 2381-2383 (2003).

[9] C. Zhang, F. Qiao, J. Wan, and J. Zi, J. Appl. Phys. 87, 3174-3176 (2000).

[10] F. Qiao, C. Zhang, J. Wan, and J. Zi, J. Appl. Phys. 87, 3698-3700 (2000).

[11] See http://ab-initio.mit.ed/mpb.

[12] L. L. Lin and Z.Y. Li, Phys. Rev. B 63, 03310 (1998).

[13] Yuan-Song Zhou, Ben-Yuan Gu, and Fu-He Wang,J. Phys. Condens. Matter 15, 4109-4118, (2003)

[14]Yuan-Song Zhou, Ben-Yuan Gu, and Fu-He Wang, The European Phys. Journal B, in press(2004).

[15] Ph. Lalanne and A. Talneau, Opt.Express 10, 354 (2002).

[16] A. Talneau, Ph. Lalanne, M. Agio and C.M. Soukoulis, Opt. Lett. 27, 1522-1524(2002).

[17] J. D. Joannopouloulos, P.R. Villeneuve, S.H. Fan, Nature 386(1997)143.

[18] J. D. Joannopouloulos, P.R. Villeneuve, S.H. Fan, Nature 387(1997) 830.

[19] A. Ta°ove, Computational Electrodynamics (Artech, Norwood, MA, 2000).

[20] J. P. Berenger, J. Comput. Phys. 114,185-200 (1994).

[21] P. Sanchis, J. Marti, A. Garcia, A. Martineand J. Blasco, Electron. Lett. 38, 961-962 (2002)